PROCEEDINGS OF THE ROYAL SOCIETY A

CrossMark click for updates

Proc. R. Soc. A (2012) **468**, 2485–2495
doi:10.1098/rspa.2011.0679
Published online 25 April 2012

Tap dance of a water droplet

By Ziqian Wang, Feng-Chao Wang and Ya-Pu Zhao*

State Key Laboratory of Nonlinear Mechanics (LNM), Institute of Mechanics, Chinese Academy of Sciences, Beijing 100190, People's Republic of China

Electro-elasto-capillarity (EEC) is a new method of droplet encapsulation controlled by an electric field. In this paper, we report some experiments, for the first time, to realize EEC under a dynamic electric field, showing the progress of electrowetting on a moving substrate. We employ the combined effects of surface tension, elastic force and Coulomb force to manipulate the flexible thin film to encapsulate and release a tiny droplet in a controllable and reversible manner. An alternating current electric field is applied to actuate the droplet and film to vibrate, as if they are dancing to a melody. We measured the frequency of the droplet and the film vibration and found that it was twice the input signal; we also carried out frequency analysis experiments. The frequency-doubling phenomenon can be explained theoretically. Our findings may offer a practical method for drug encapsulation and for the actuation of microelectromechanical system devices.

Keywords: electro-elasto-capillarity; elasto-capillarity; frequency doubling; electrowetting on a moving substrate

1. Introduction

Small things are usually more difficult to control and manipulate than normal-sized objects; for example, we can easily pour a litre of water into a canteen and carry it, but it is difficult to find a suitable canteen for a 1 microlitre drop (the diameter is no larger than 1 mm). Scientists have employed capillary force (Jiang & Kiørboe 2011; Voise *et al.* 2011) and electrowetting (De Gennes 1985; De Mello 2001; Li & Fontelos 2003; Heikenfeld & Steckl 2005; Berthier 2008; Ko *et al.* 2008; Lu *et al.* 2008; Fan *et al.* 2009; Kwon *et al.* 2009) to manipulate such small objects. However, during the process of manipulation, the droplet is usually exposed to the environment, either liquid or air. In such an environment, contamination and evaporation of the liquid cannot be eliminated, which usually results in the failure of biological or chemical experiments. Consequently, a proper 'container' for a small droplet is required in microelectromechanical systems (MEMS), bio-engineering, chemistry and physics. In our experiments, we have not only found a 'proper container' for a 1 microlitre droplet, but also 'trained' the drop to become a 'tap dancer'.

*Author for correspondence (yzhao@imech.ac.cn).

Electronic supplementary material is available at http://dx.doi.org/10.1098/rspa.2011.0679 or via http://rspa.royalsocietypublishing.org.

Received 15 November 2011
Accepted 27 March 2012

It is reported that, driven by capillary force, an elastic film tends to spontaneously wrap a droplet when the size of the droplet exceeds a characteristic length L_{EC} (Bico *et al.* 2004; Patra *et al.* 2007; Py *et al.* 2007; Guo *et al.* 2009; Roman & Bico 2010). This phenomenon is called capillary origami, or elasto-capillarity (EC), and L_{EC} is expressed as

$$L_{\mathrm{EC}} = \sqrt{\frac{B}{(1+\cos\theta_{\mathrm{a}})\gamma_{\mathrm{lv}}}}, \tag{1.1}$$

where B is the stiffness of the film, γ_{lv} is the liquid–vapour interface tension and θ_{a} is the contact angle of the droplet on the film. Because EC is a possible means of manipulating a tiny amount of a liquid, it has been the subject of much interest among scientists in bio-medicine (De Mello 2001), physics (De Gennes 1985; Heikenfeld & Steckl 2005) and chemistry (Kwon *et al.* 2009). It has been reported that polydimethylsiloxane (PDMS) film and a single crystallized silicon film are able to wrap a droplet (Guo *et al.* 2009). It has also been forecast that graphene film is capable of wrapping a nanoscale droplet (Patra *et al.* 2007), by molecular dynamics (MD) simulations. As a result, EC has become an important candidate for encapsulation of small amounts of liquid and an actuation method for microstructures (Shanahan 1985, 1987) since its emergence.

However, at micro- or nanoscale, the surface tension is usually a more dominant interaction in liquids than the elastic force, gravitational force, etc. Once wrapped by a film, the droplet will not be released, unless the liquid is evaporated. Thus, a controllable and reversible manner of encapsulating and releasing a droplet is strongly required by the application fields. Yuan & Zhao's (2010) work forecasts that, under an electric field, graphene film can unwrap a nanoscale droplet, by MD simulations, which is known as electro-elasto-capillarity (EEC). It is also reported that PDMS film can release microlitre-scale droplets under an electric static field (Pineirua *et al.* 2010).

In this paper, EEC under direct current (DC) and alternating current (AC) electric field has been realized experimentally. We found that, provoked by an AC voltage, the droplet and elastic film start to vibrate, just like a tap dancer dancing to music. We also found that the dancer's tune is one octave higher than the music input, and the movement of the dancer seems to be more intensive when the music is set at some specific notes.

2. Results and discussions

(*a*) *Experimental set-up*

In the experiments, one droplet of salty water ($0.1\,\mathrm{mol\,l^{-1}}$ KCl solution) was placed upon a slice of flexible PDMS film (figure 1*a*). As a result of the vertical component of the liquid–vapour interface tension, the thin film bent upwards and wrapped around the droplet when the size of drop was larger than L_{EC}. The PDMS film was placed on a superhydrophobic surface. After the droplet was wrapped completely by the film, one Pt wire electrode was inserted into the drop at the apex. The other electrode was set beneath the superhydrophobic substrate. A schematic of the experiments is shown in figure 1*b*. The superhydrophobic substrate was the insulator, which isolated the encapsulated droplet from the

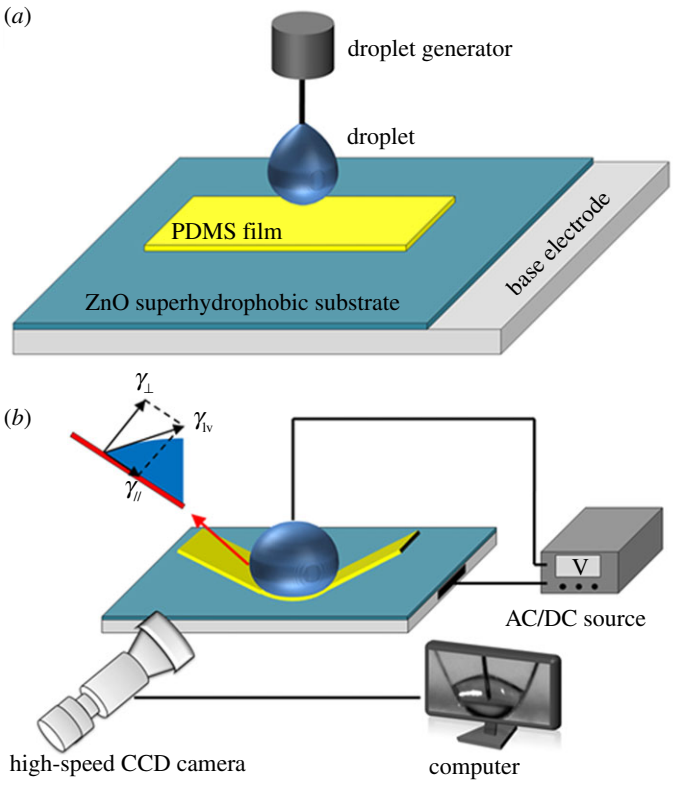

Figure 1. Schematic of experiments. (*a*) A droplet is placed upon a slice of flexible elastic PDMS film. The film will be bent or even wrap around the droplet because of the vertical component of the surface tension of the droplet. (*b*) With an increase in voltage, the film tends to unwrap the droplet.

electric current and provided a low adhesion force to the PDMS film at the same time. Because of the low adhesion force, the PDMS film was able to wrap the droplet spontaneously and repeatedly.

The wrapped droplet, together with the electrode, was placed on the stage of a DataPhysics OCA-20 contact angle meter. A CCD camera that can capture 1000 frames of pictures every second was set on the same horizontal plane as the droplet to take a side view of the wrapped droplet. The thickness of the PDMS film (Sylgard 184, Dow Corning, USA) used in the experiments was 70 µm (Dai & Zhao 2007). The PDMS film was cut into 5 × 1 mm rectangular slices and moved to the superhydrophobic surface.

Both electrodes were connected to a home-designed voltage source, which can provide both AC and DC voltage from 0 to 6000 V (r.m.s. value for the AC mode). The frequency of the AC voltage can be set from 20 to 400 Hz.

(*b*) *Tap dance of a droplet*

We first applied DC voltage to the droplet. While the voltage is being applied between the droplet and the base electrode, the entire system could be considered as a capacitor. The upper electrode was the droplet; the lower electrode was

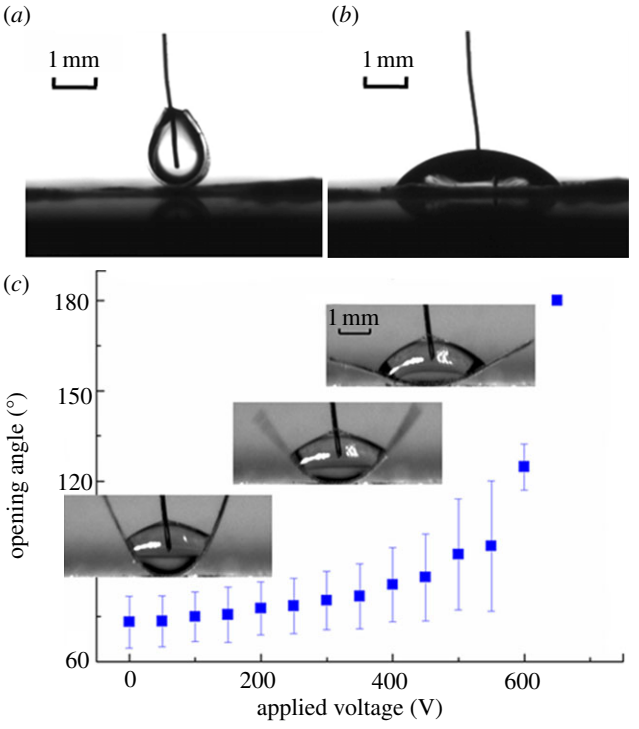

Figure 2. EEC under DC voltage. (*a*) When the voltage is 0, no Coulomb force will pull the film to unwrap the drop; (*b*) when the voltage reaches the critical value, the film completely unwraps the drop; (*c*) while the voltage is increases, the opening angle increases and finally reaches 180°.

the substrate and the dielectric film was composed of PDMS film, air and superhydrophobic film. With an increase in voltage, the flexible PDMS film was pulled down, towards the substrate, as shown in figure 2*a*,*b*. When the voltage reached a certain value, the pull-in voltage, the wrapped droplet was completely released and the film was entirely spread over the superhydrophobic surface (figure 2*c*). When the electric field was removed, the PDMS film wrapped the drop again. So the process is controllable and reversible.

Then we applied AC voltage to the droplet and the substrate. As a consequence of the AC voltage, the system composing the droplet and film starts to vibrate. Under the high-speed CCD camera, the vibration of the droplet makes it look as though it is 'tap dancing' and the flexible film is its 'dancing skirt'. As shown in figure 3, the droplet was dancing to the rising and falling of the voltage (electronic supplementary material, video S1). When the voltage reached its peak, the film released the droplet to the largest scale. If the voltage was as high as the pull-in voltage described earlier, the film completely adhered to the superhydrophobic surface.

There are two reasons for the release of the droplet, the first is the increase in the Coulomb force. As the voltage increases, the Coulomb force between the droplet and the substrate gets larger. The capacitor of the drop and the substrate acts as a microcapacitor actuator. When the voltage reaches the pull-in voltage, the PDMS film will be pulled-in to the substrate and the droplet released.

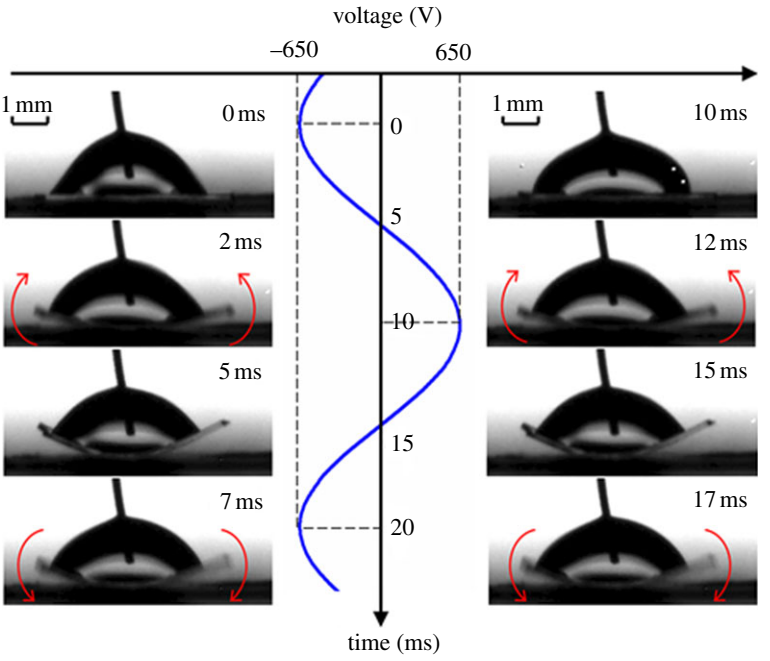

Figure 3. When AC voltage is applied, the film starts to vibrate like a dancer. The opening angle reaches its peak when the voltage reaches the highest point.

The second reason is the electrowetting effect on a non-fixed dielectric film, where the dielectric film includes the PDMS film, the superhydrophobic layer and the air between them. When an electric field is applied, the contact angle decreases as the voltage rises. The vertical component of the liquid–vapour interface tension is expressed as $\gamma_\perp = \gamma_{\mathrm{lv}} \sin \theta_{\mathrm{a}}$. Because θ_{a} is measured as 90°, when θ_{a} decreases, $\gamma_\perp$ also decreases. In our experiments, the relationship between the contact angle θ_{a} and the applied voltage U is shown in the Lippmann–Young equation

$$\cos \theta_{\mathrm{a}} = \cos \theta_0 + \frac{C_{\mathrm{cap}} U^2}{2\gamma_{\mathrm{lv}}}, \tag{2.1}$$

where θ_{a} is the macroscopic contact angle, θ_0 is the intrinsic contact angle of the substrate, C_{cap} is the capacitance of the system and U is the voltage. The direction of the vertical component of the surface tension is upwards, and the direction of the Coulomb force is downwards. Under the combined influence of the two forces, the PDMS film unwraps the droplet.

When applied with a DC electric field, the droplet significantly spreads out on the surface of the PDMS film because of the Maxwell stress induced by a high voltage (Dai & Zhao 2007). The energy dissipation caused by contact angle hysteresis (CAH) is notable. As discussed in our further research, the work of adhesion w_{A} from CAH is expressed as $w_{\mathrm{A}} = \gamma_{\mathrm{lv}}(\cos \theta_{\mathrm{rec}} - \cos \theta_{\mathrm{adv}})$, where θ_{rec} refers to the receding angle and θ_{adv} refers to the advancing angle (Wang & Zhao, in press). Furthermore, the large deformation of the film and multi-field will also complicate the analysis of the system. However, during the tap dance of the droplet, we applied a lower voltage to avoid adhesion of the PDMS wings

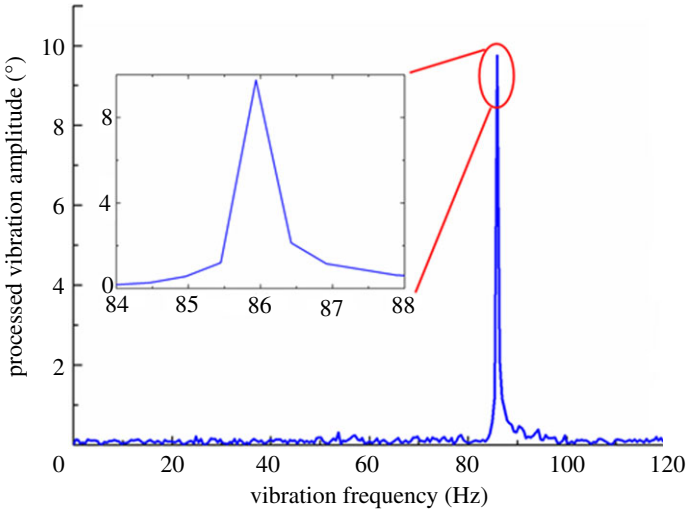

Figure 4. The FFT result of the opening angle information. When the frequency of the input voltage is 43 Hz, the vibrating rate is 86 Hz.

and substrate. Consequently, the movement of the contact line is not visible in the experiments (shown in the electronic supplementary material, video S1) and the hysteresis is negligible. In this paper, we focus on the frequency effect of the system.

(*c*) *Frequency-doubling effect*

Because the droplet is a dancer, we set music tunes as the signal input. The input signal was set to be sub-contra F (fa ∼ 43 Hz) and the voltage to be 340 V. The voltage was set to be lower than the pull-in voltage so that the adhesion force of the superhydrophobic surface did not influence the experiments. When the droplet started to 'dance', we captured the droplet motion by high-speed CCD camera. We developed a program to analyse this progress. Every frame of the movie was processed and the opening angle information of the system was obtained every 0.001 s. Then the opening angle data were fast Fourier transformed into the frequency domain, as shown in figure 4. From the frequency domain curve of the experiments, we discovered that the vibration is contra F (fa ∼ 86 Hz), i.e. twice that of the input frequency. It is interesting that, while the droplet was dancing, the tune of the dance was one octave higher than the input (as in music, the tone being one octave higher means that the frequency was doubled). To determine the reason for the frequency-doubling effect of the vibration, we analysed the phenomenon as follows.

For the analysis of the dynamic vibration of EEC induced by the applied AC voltage, a simplified two-dimensional model was considered, which is shown in figure 5*a*. The PDMS film of width w and length l was divided into two parts, the arc pedestal of length l_1 in which the bending deflection dominates and the lateral wings with a length l_2 where the vibration dominates. Thus, we can obtain $l = l_1 + 2l_2$. The opening angle θ is defined by the angle between the two PDMS

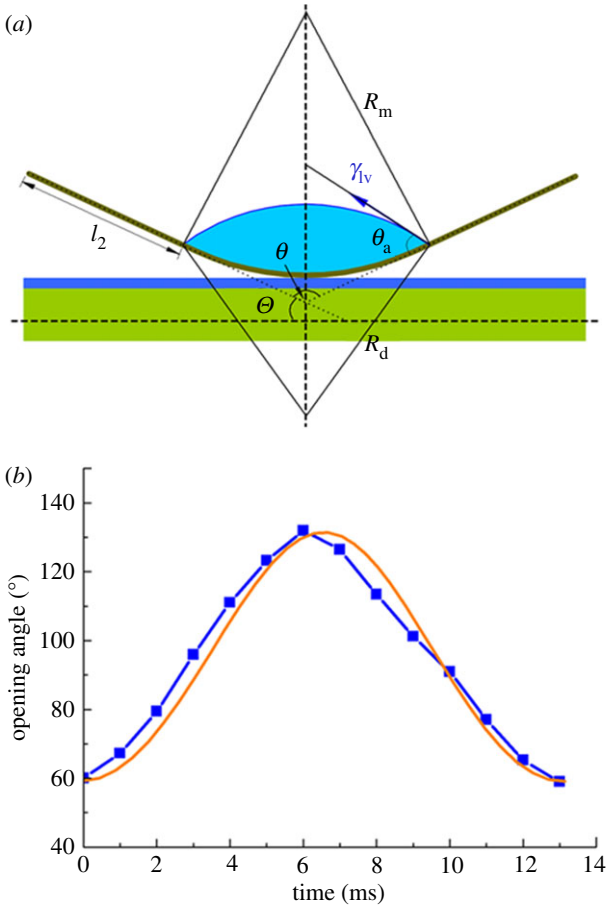

Figure 5. The numerical solution (solid line) of the opening angle of the PDMS film. The input frequency of the AC voltage is 38 Hz compared with those of the experiments (squares).

wings. $\theta = \pi - 2\Theta$ and Θ is the angle between the PDMS wing and the substrate. The total kinetic energy of the two lateral PDMS wings is given by

$$E_k = I\dot{\Theta}^2, \tag{2.2}$$

where I is the moment of inertia of each wing.

The components that contribute to the potential energy of the system include the elastic bending energy of the arc PDMS pedestal, the interfacial energy of the liquid droplet and the electric energy that is stored in the capacitor. The gravitational–potential energy can be neglected because the scale of the droplets used in our experiments is smaller than the capillary length $l_c = \sqrt{\gamma_{lv}/\rho g}$ (2.7 mm for water), where ρ is the density of the liquid and g is the gravitational acceleration.

The bending energy of the PDMS pedestal is

$$E_b = \frac{1}{2}\frac{Bl_1 w}{R_m^2}, \tag{2.3}$$

where $B = Eh^3/[12(1-\nu^2)]$ is the bending stiffness of the PDMS membrane with a thickness of h. E and ν are Young's modulus and Poisson's ratio of PDMS (Freund 1990; Pineirua *et al.* 2010), respectively. $R_\mathrm{m} = l_1/2\Theta$ is the radius of curvature of the arc PDMS pedestal.

During the vibration, the contact angle θ_a varies over time and its frequency is equal to that of the vibration of the PDMS wings. The surface energy of the liquid droplet is given by

$$E_\mathrm{s} = 2\gamma_\mathrm{lv} \mathrm{w} R_\mathrm{d}(\theta_\mathrm{a} - \Theta), \tag{2.4}$$

where R_d is the radius of curvature of the liquid droplet. From the analysis of the geometrical relationship, we can obtain $R_\mathrm{d} = R_\mathrm{m} \sin\Theta/\sin(\theta_\mathrm{a} - \Theta)$. According to the experimental results, $\Delta = \theta_\mathrm{a} - \Theta$ is an approximate constant of $\pi/12$.

The total electric energy stored in the capacitor is expressed by (Ida 2004; Pineirua *et al.* 2010)

$$E_\mathrm{e} = -\pi\varepsilon w \left(\frac{R_\mathrm{m}}{2h'}\right)^{1/2} V_0^2 \sin^2\omega t, \tag{2.5}$$

where ε is the dielectric constant, h' is the gap thickness and $V = V_0 \sin\omega t$ is the applied AC voltage.

To include the damping effect, we introduce a dissipation function D, in the following form:

$$D = \frac{1}{2} C\dot{\Theta}^2, \tag{2.6}$$

where C is the damping coefficient in the physical system.

The Lagrangian equation for this system with damping can be written as

$$\frac{\mathrm{d}}{\mathrm{d}t}\frac{\partial L}{\partial\dot{\Theta}} - \frac{\partial L}{\partial\Theta} + \frac{\partial D}{\partial\dot{\Theta}} = 0, \tag{2.7}$$

where $L = E_\mathrm{k} - E_\mathrm{b} - E_\mathrm{s} - E_\mathrm{e}$ is the Lagrangian.

Then, the governing equation for the vibration of the lateral PDMS wings can be derived by using equation (2.7),

$$\underbrace{2I\frac{\mathrm{d}^2\Theta}{\mathrm{d}t^2}}_{\text{kinetic energy}} = -\underbrace{\frac{4Bw\Theta}{l_1}}_{\text{bending energy}} - \underbrace{\frac{\gamma_\mathrm{lv} w l_1 \Delta}{\sin\Delta}\frac{\Theta\cos\Theta - \sin\Theta}{\Theta^2}}_{\text{surface energy}} - \underbrace{\frac{\pi\varepsilon w\sqrt{l_1/h'}\,V_0^2\sin^2\omega t}{4\Theta^{3/2}}}_{\text{electric energy}} - \underbrace{C\frac{\mathrm{d}\Theta}{\mathrm{d}t}}_{\text{dissipation}}. \tag{2.8}$$

The numerical solution of equation (2.8) is shown in figure 5*b*, under the initial conditions $\Theta(t=0) = \pi/3$ and $\Theta_t(t=0) = 0$, which were estimated from the experimental data. From figure 5*b*, we can see that our theoretical model captures the frequency doubling of the AC voltage-induced vibration, which indicates that the electric energy term consisting of $\sin^2\omega t$ may be dominant in the governing equation. Also we can see that the theoretical data show good agreement with the experimental results.

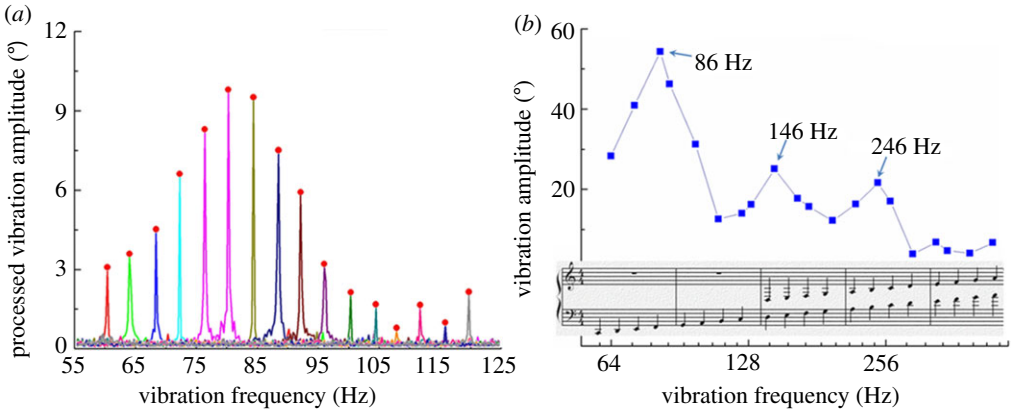

Figure 6. A frequency analysis of EEC under AC voltage. (*a*) As the sweep input frequency is set from 30 to 60 Hz, the resonance peak appears at 40 Hz input (80 Hz vibration). (*b*) When the set input signal is the same as the scale on a piano keyboard, three resonance peaks can be seen, at 86, 146 and 246 Hz (vibration rate), respectively.

(*d*) *Frequency analysis*

The doubling phenomenon occurred not only at one specific frequency but also in all of the experiments. We swept the input frequency from 30 to 60 Hz, with a constant interval of 2 Hz and a constant voltage of 340 V, and the vibration amplitude of the system is shown in figure 6*a*. The vibrating frequency was doubled, without exception, and one resonance peak was observed at 40 Hz (the input frequency was 40 Hz and the vibration rate was 80 Hz). This means that the characteristic time of the system is 12.5 ms.

The characteristic time of the vibration of a free droplet is estimated according to Rayleigh's solution to the free vibration of droplet (Feng & Zhao 2008),

$$T = \frac{\pi}{4}\sqrt{\frac{\rho d^3}{\gamma_{\mathrm{lv}}}}, \tag{2.9}$$

where d is the diameter of the droplet. In the experiment, the size of droplet d is about 2 mm, the surface tension γ_{lv} is $72 \times 10^{-3}\,\mathrm{N\,m^{-1}}$ at room temperature and the density is $1 \times 10^{3}\,\mathrm{kg\,m^{-3}}$. So the characteristic time of the droplet is calculated to be about 8.3 ms. The theoretical value and the measured value are of the same order of magnitude. The error is possibly introduced by the additional mass of flexible PDMS film and the adhesion force of the superhydrophobic surface and PDMS film. Both of these will prolong the vibration period.

In order to obtain more information, we swept the input signal in the scale of a piano keyboard, from 20 to 230 Hz (figure 6*b*). Two weaker resonance peaks were found at 73 and 123 Hz of input signal (146 and 246 Hz vibration rate, respectively). These two peaks are believed to be high modes of the system.

3. Conclusions

For the first time, EEC under dynamic electric field is realized in experiments. This progress can also be considered as electrowetting progress on a moving

substrate. Actuated by Coulomb force and surface tension, an encapsulated water droplet can be released, controllably and reversibly. In an AC driving electric field, the droplet and thin film vibrate as if they are dancing. The present results show that the vibration frequency of the droplet and thin film is twice that of the driving signal. The vibration intensity of the system produces several resonance peaks, at specific input frequencies. This controllable and reversible method of unwrapping a droplet will offer a possible way of drug encapsulation and microdevice actuation.

4. Material and methods

(*a*) *Preparation of the flexible polydimethylsiloxane thin film*

The PDMS (Sylgard 184, Dow Corning, USA) used in the experiments was prepared in the following way: the mass ratio of the base to curing was 10 : 1, after baking at 150°C for 20 min until the PDMS was cured. PDMS was spin coated on the surface of indium tin oxide glass at 1000 r.p.m., and the thickness was 70 μm (Dai & Zhao 2007). Then, the PDMS film was cut into 5×1 mm rectangular slices and peeled off from the substrate.

(*b*) *Fabrication of the zinc oxide superhydrophobic surface*

The nanostructured ZnO material was first synthesized via a simple catalyst-free CVD method (Bhushan *et al.* 2007; Wang *et al.* 2010, 2011). In the experiment, 2.0 g Zn powder (99.999%) was heated up to 640°C under a 300 standard cubic centimetres per minute (SCCM) Ar gas flow. Then, 20 SCCM O_2 gas flow was introduced into the system and maintained for 20 min. After the ZnO powder was fabricated, it was dispersed in ethyl alcohol under supersonic waves for 20 min, and repeated four times. The ZnO powder was then dispersed on a half-cured PDMS film (the process is the same as that described in the previous paragraph but it was baked for only 5 min, so that the mixture was not completely cured). Finally, deionized water was used to remove the excess ZnO powder. The ZnO surface is superhydrophobic; therefore, the contact angle of water reaches over 159° and the CAH is about $3.1 \pm 0.3°$. The adhesion force between the superhydrophobic surface and the flexible PDMS film is estimated to be $6\,\mathrm{N\,m^{-2}}$.

This work was jointly supported by the National Natural Science Foundation of China (NSFC; grant no. 11072244), the Key Research Program of the Chinese Academy of Sciences (grant no. KJZD-EW-M01) and the Instrument Developing Project of the Chinese Academy of Sciences (grant no. Y2010031).

References

Berthier, J. 2008 *Microdrops and digital microfluidics*. Norwich, NY: William Andrew.

Bhushan, B., Nosonovsky, M. & Jung, Y. C. 2007 Towards optimization of patterned superhydrophobic surfaces. *J. R. Soc. Interface* **4**, 643–648. (doi:10.1098/rsif.2006.0211)

Bico, J., Roman, B., Moulin, L. & Boudaoud, A. 2004 Elastocapillary coalescence in wet hair. *Nature* **432**, 690. (doi:10.1038/432690a)

Dai, W. & Zhao, Y. P. 2007 The nonlinear phenomena of thin polydimethylsiloxane (PDMS) films in electrowetting. *Int. J. Nonlinear Sci. Numer. Simul.* **4**, 519–526.

De Gennes, P. G. 1985 Wetting-statics and dynamics. *Rev. Mod. Phys.* **57**, 827–863. (doi:10.1103/RevModPhys.57.827)

De Mello, A. J. 2001 DNA amplification: does 'small' really mean 'efficient'? *Lab Chip* **1**, 24N–29N. (doi:10.1039/b109740g)

Fan, S. K., Hsieh, T. H. & Lin, D. Y. 2009 General digital microfluidic platform manipulating dielectric and conductive droplets by dielectrophoresis and electrowetting. *Lab Chip* **9**, 1236–1242. (doi:10.1039/b816535a)

Feng, J. T. & Zhao, Y. P. 2008 Experimental observation of electrical instability of droplets on dielectric layer. *J. Phys. D: Appl. Phys.* **5**, 052004. (doi:10.1088/0022-3727/41/5/052004)

Freund, L. 1990 *Dynamic fracture mechanics*. Cambridge, MA: Cambridge University Press.

Guo, X. Y., Li, H., Ahn, B. Y., Duoss, E. B., Hsia, K. J., Lewis, J. A. & Nuzzo, R. G. 2009 Two- and three-dimensional folding of thin film single-crystalline silicon for photovoltaic power applications. *Proc. Natl Acad. Sci. USA* **106**, 20 149–20 154. (doi:10.1073/pnas.0907390106)

Heikenfeld, J. & Steckl, A. J. 2005 High-transmission electrowetting light valves. *Appl. Phys. Lett.* **86**, 151121. (doi:10.1063/1.1901816)

Ida, N. 2004 *Engineering electromagnetics*, 2nd edn. New York, NY: Springer.

Jiang, H. & Kiørboe, T. 2011 The fluid dynamics of swimming by jumping in copepods. *J. R. Soc. Interface* **8**, 1090–1103. (doi:10.1098/rsif.2010.0481)

Ko, S. H., Lee, H. & Kang, K. H. 2008 Hydrodynamic flows in electrowetting. *Langmuir* **24**, 1094–1101. (doi:10.1021/la702455t)

Kwon, Y., Patankar, N., Choi, J. & Lee, J. 2009 Design of surface hierarchy for extreme hydrophobicity. *Langmuir* **25**, 6129–6136. (doi:10.1021/la803249t)

Li, J. & Fontelos, M. A. 2003 Drop dynamics on the beads-on-string structure for viscoelastic jets: a numerical study. *Phys. Fluids* **15**, 922–937. (doi:10.1063/1.1556291)

Lu, H. W., Bottausci, F., Fowler, J. D., Bertozzi, A. L., Meinhart, C. & Kim, C. J. 2008 A study of EWOD-driven droplets by PIV investigation. *Lab Chip* **8**, 456–461. (doi:10.1039/b717141b)

Patra, N., Wang, B. Y. & Kral, P. 2007 Nanodroplet activated and guided folding of graphene nanostructures. *Nano Lett.* **9**, 3766–3771. (doi:10.1021/nl9019616)

Pineirua, M., Bico, J. & Roman, B. 2010 Capillary origami controlled by an electric field. *Soft Matter* **6**, 4491–4496. (doi:10.1039/c0sm00004c)

Py, C., Reverdy, P., Doppler, L., Bico, J., Roman, B. & Baroud, C. N. 2007 Capillary origami: spontaneous wrapping of a droplet with an elastic sheet. *Phys. Rev. Lett.* **98**, 156103. (doi:10.1103/PhysRevLett.98.156103)

Roman, B. & Bico, J. 2010 Elasto-capillarity: deforming an elastic structure with a liquid droplet. *J. Phys. Condens. Mat.* **22**, 493101. (doi:10.1088/0953-8984/22/49/493101)

Shanahan, M. 1985 Contact-angle equilibrium on thin elastic solids. *J. Adhes.* 18, 247–267. (doi:10.1080/00218468508080461)

Shanahan, M. 1987 Equilibrium of liquid-drops on thin plates: plate rigidity and stability considerations. *J. Adhes.* **20**, 261–274. (doi:10.1080/00218468708074946)

Voise, J., Schindler, M., Casas, J. & Raphaël, E. 2011 Capillary-based static self-assembly in higher organisms. *J. R. Soc. Interface* **8**, 1357–1366. (doi:10.1098/rsif.2010.0681)

Wang, F. C. & Zhao, Y. P. In press. Contact angle hysteresis at the nanoscale: a molecular dynamics simulation study. *J. Adhes. Sci. Technol.*

Wang, B. B., Feng, J. T., Zhao, Y. P. & Yu, T. X. 2010 Fabrication of novel superhydrophobic surfaces and water droplet bouncing behavior. I. Stable ZnO-PDMS superhydrophobic surface with low hysteresis constructed using ZnO nanoparticles. *J. Adhes. Sci. Technol.* **24**, 2693–2705. (doi:10.1163/016942410X508244)

Wang, B. B., Zhao, Y. P. & Yu, T. X. 2011 Fabrication of novel superhydrophobic surfaces and droplet bouncing behavior. II. Water droplet impact experiment on superhydrophobic surfaces constructed using ZnO nanoparticles. *J. Adhes. Sci. Technol.* **25**, 93–108. (doi:10.1163/016942410X501115)

Yuan, Q. Z. & Zhao, Y. P. 2010 Precursor film in dynamic wetting, electrowetting, and electro-elasto-capillarity. *Phys. Rev. Lett.* **24**, 246101. (doi:10.1103/PhysRevLett.104.246101)